Identification and characterization of abrupt changes in the land uptake of carbon

Claudie Beaulieu,[1] Jorge L. Sarmiento,[1,2] Sara E. Mikaloff Fletcher,[3] Jie Chen,[4] and David Medvigy[1,2]

Received 17 December 2010; revised 17 June 2011; accepted 6 November 2011; published 19 January 2012.

[1] A recent study of the net land carbon sink estimated using the Mauna Loa, Hawaii atmospheric CO_2 record, fossil fuel estimates, and a suite of ocean models suggests that the mean of the net land carbon uptake remained approximately constant for three decades and increased after 1988/1989. Due to the large variability in the net land uptake, it is not possible to determine the exact timing and nature of the increase robustly by visual inspection. Here, we develop a general methodology to objectively determine the nature and timing of the shift in the net land uptake based on the Schwarz Information Criterion. We confirm that it is likely that an abrupt shift in the mean net land carbon uptake occurred in 1988. After taking into account the variability in the net land uptake due to the influence of volcanic aerosols and the El Niño Southern Oscillation, we find that it is most likely that there is a remaining step increase at the same time (p-values of 0.01 and 0.04 for Mauna Loa and South Pole, respectively) of about 1 Pg C/yr. Thus, we conclude that neither the effect of volcanic eruptions nor the El Niño Southern Oscillation are the causes of the sudden increase of the land carbon sink. By also applying our methodology to the atmospheric growth rate of CO_2, we demonstrate that it is likely that the atmospheric growth rate of CO_2 exhibits a step decrease between two fitted lines in 1988–1989, which is most likely due to the shift in the net land uptake of carbon.

Citation: Beaulieu, C., J. L. Sarmiento, S. E. Mikaloff Fletcher, J. Chen, and D. Medvigy (2012), Identification and characterization of abrupt changes in the land uptake of carbon, *Global Biogeochem. Cycles*, *26*, GB1007, doi:10.1029/2010GB004024.

1. Introduction

[2] Ocean and terrestrial sinks remove more than half of the anthropogenic CO_2 emitted to the atmosphere, leaving less CO_2 to accumulate in the atmosphere. Changes in the efficiency of these sinks could have a substantial impact on the rate of climate change [e.g., *Raupach*, 2011]. Thus, understanding of the temporal evolution of these sinks is important for the Earth's carbon cycle and climate system.

[3] *Sarmiento et al.* [2010] suggested that an abrupt shift in the net land carbon sink, estimated as the balance between the fossil fuel emissions, the growth rate of atmospheric CO_2 at Mauna Loa and the ocean carbon uptake estimated from ocean models, occurred in the late 1980s (Figure 1). In their analysis, the land carbon uptake appears to have remained relatively constant (with a mean of 0.27 Pg C/yr) from 1960 to 1988 and to have increased after 1988 (to a mean of 1.15 Pg C/yr). However, they also pointed out that the nature of the increase is difficult to detect given the short period of observations (1960–2008), and the high variability and uncertainty in the observations.

[4] The large inter-annual variability in the land-atmosphere carbon uptake complicates both the detection and attribution of abrupt changes. For example, *Sarmiento et al.* [2010] visually identified a 1988/89 shift in the mean uptake. This identification, however, is ambiguous given the variability in the land uptake. Other classes of shifts (e.g., shifts in the mean and in the variance, a long-term linear trend or a shift in the long term linear trend) may or may not better explain the data, but these possibilities were not investigated by *Sarmiento et al.* [2010]. Furthermore, it is well known that the variability of land uptake is strongly influenced by ENSO [*Thoning et al.*, 1989; *Keeling et al.*, 1995; *Jones and Cox*, 2005; *Raupach et al.*, 2008; *Le Quéré et al.*, 2009] and large volcanic eruptions [*Jones and Cox*, 2001; *Sarmiento et al.*, 2010]. The extent to which a 1988/89 shift can be attributed to these factors, to long-term (or quasi-decadal) change in the solar irradiance reaching the Earth's surface [*Sarmiento et al.*, 2010], or to other factors is not currently known.

[1]Program in Atmospheric and Oceanic Sciences, Princeton University, Princeton, New Jersey, USA.
[2]Department of Geosciences, Princeton University, Princeton, New Jersey, USA.
[3]National Institute of Water and Atmospheric Research, Wellington, New Zealand.
[4]Department of Mathematics and Statistics, University of Missouri at Kansas City, Kansas City, Missouri, USA.

0886-6236/12/2010GB004024

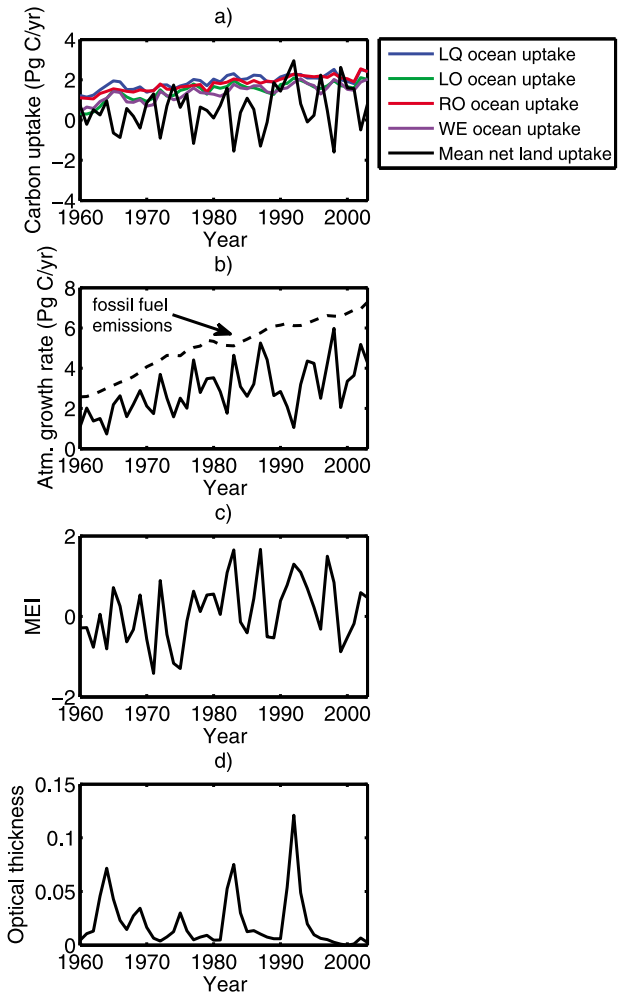

Figure 1. Net land carbon uptake, its components and its covariate effects: (a) the ocean uptake estimated from four ocean models (LQ = *Le Quéré et al.* [2007], LO = *Lovenduski et al.* [2008], RO = *Rodgers et al.* [2008], and WE = *Wetzel et al.* [2005]) and the mean of the four net land uptake time series obtained with the four ocean uptake estimates, (b) the atmospheric growth rate at Mauna Loa and the fossil fuel emissions (dotted line), (c) the Multivariate ENSO Index, and (d) the stratospheric aerosol optical thickness. The references are presented in the data section.

[5] Given the importance of such a shift for the Earth's carbon cycle, we here conduct a more rigorous statistical analysis of the temporal shifts in the net land carbon uptake. In particular, we utilize objective change point detection in lieu of the visual method used by *Sarmiento et al.* [2010]. In a general sense, a change point can be viewed as a time instance at which the parameters of a statistical distribution or a statistical model change. Thus, most change point detection techniques identify the most likely time for a shift and determine whether or not this shift occurred by comparing a model with a shift (or a change point model) to a simpler model without a shift [e.g., *Brown et al.*, 1975; *Solow*, 1987; *Jandhyala and MacNeill*, 1991; *Lund et al.*, 2007]. An information criterion is then used to determine which model is more appropriate [*Chen and Gupta*, 1997, 1999, 2000]. This informational approach can also be useful to discriminate between several change point models with different types of changes (shift in the mean, shift in the parameters of a linear regression model, etc.), as it is generally used for model selection.

[6] In this study, we develop a general methodology based on the Schwarz Information Criterion (SIC) for model selection [*Schwarz*, 1978]. We use this criterion to detect the time of abrupt changes in time series and to discriminate between no-change, gradual change and abrupt change. We verify the conclusions of *Sarmiento et al.* [2010] by fitting several types of models (shift in the mean and shift in the parameters of a linear regression model) to the net land uptake estimated using the growth rate of atmospheric CO_2 at Mauna Loa and South Pole from the Scripps Institution of Oceanography (SIO) observation network, the two longest atmospheric CO_2 records available. Monte Carlo simulations are used to quantify the significance in our results. We repeat this analysis for all of the observing stations with publicly available atmospheric CO_2 data starting no later than in 1980. We also investigate whether the shift in the net land uptake is related to the Mount Pinatubo eruption or to changes in ENSO variability by including these two covariate effects in the multiple linear regression models. Furthermore, we investigate if a similar shift is detected in the CO_2 atmospheric growth rate to confirm the analysis performed on the net land uptake.

[7] The rest of this paper is organized as follows: section 2 presents the data used in this study. The methodology used to detect change points and to discriminate between several models and the Monte Carlo simulation scheme are described in section 3, and the results are presented in section 4. A discussion about the limitations of these results and the potential of application of this methodology to different problems is presented in section 5 and the conclusions are presented in section 6. The details of the change point detection and model selection technique and additional evidence for a shift in the net land uptake are presented in Appendices A and B.

2. Data and Flux Estimates

2.1. Land and Ocean Uptake of Carbon

[8] Following *Sarmiento et al.* [2010], the net land uptake of CO_2 is computed as the difference between the fossil fuel emissions, the atmospheric growth rate and the ocean uptake. The net land carbon sink, as opposed to the land carbon sink, does not require specification of land use emissions (Net land carbon sink = land carbon sink – land use emissions). The emissions from land use were not included because they are highly uncertain and are thought to have remained approximately constant from 1959 to 2006 [*Canadell et al.*, 2007]. Several versions of the net land uptake were computed using the atmospheric CO_2 growth rate at Mauna Loa and South Pole (described in section 2.2). Additional stations with shorter records were also used and are presented in Appendix B. The ocean uptake is estimated using four different ocean models to reflect its uncertainty: *Le Quéré et al.* [2007], *Lovenduski et al.* [2008], *Rodgers et al.* [2008] and *Wetzel et al.* [2005]. These ocean uptake estimates are presented in Figure 1a. We computed the net

land uptake with these four ocean estimates and averaged it from 1960 to 2003 (the common period of observations and ocean model simulations) to perform our analyses (Figure 1a). The net land carbon sink and ocean uptake discussed in the paper are all in terms of carbon storage rather than flux. A comparison of our storage changes with air-to-sea or land to atmosphere fluxes should require adding the background natural fluxes due to weathering and related processes [*Sarmiento and Sundquist*, 1992].

2.2. Atmospheric Growth Rate and Fossil Fuel Emissions

[9] In this study, we primarily use the monthly CO_2 concentration observations at Mauna Loa and the South Pole from the SIO network [*Keeling et al.*, 2001] (available at http://scrippsco2.ucsd.edu/data/atmospheric_co2.html) because they are the two longest records available and the most commonly used to represent the global CO_2 concentrations. The annual atmospheric growth rate was computed annually as described on the NOAA-ESRL website (http://www.esrl.noaa.gov/gmd/ccgg/trends/#mlo_full):

$$agr_t = 2.1276(\text{Pg C/ppm}) \cdot (\bar{c}_t - \bar{c}_{t-1}) \quad (1)$$

where agr_t is the atmospheric growth rate in Pg C/year for year t and $\bar{c}_t$ is the mean CO_2 concentration in ppm, for months November–February centered around January 1st of year t. The CO_2 concentration is corrected for the seasonal cycle, by subtracting a 4-harmonic fit with a linear gain factor from the data [*Keeling et al.*, 2001]. The fossil fuel and cement emissions for 1958–2005 were obtained from *Boden et al.* [2009] (available at http://cdiac.ornl.gov/trends/emis/tre_glob.html). These estimates are based on the energy statistics from each country. Figure 1b presents the fossil fuel emissions and the atmospheric growth rate computed using the Mauna Loa observations from SIO.

2.3. Covariate Effects

[10] To first order, the net land uptake variability can be explained by ENSO and volcanic eruptions [*Sarmiento et al.*, 2010]. In order to model these factors, the Multivariate ENSO Index was used as a proxy for the ENSO-related variability from the National Oceanic and Atmospheric Administration–Climate Diagnostics Center (NOAA-CDC) [*Wolter and Timlin*, 1993, 1998] (available at http://www.cdc.noaa.gov/people/klaus.wolter/MEI/table.html). Many other ENSO indices were considered in a preliminary analysis. However, most of them are based on sea surface temperatures and there is no clear consensus in the scientific community as to which of these indices is the best characterization of ENSO [*Hanley et al.*, 2003]. The MEI was chosen because it combines the significant features of six observables over the tropical Pacific: sea level pressure, zonal and meridional components of the surface wind, sea surface temperature, surface air temperature and total cloudiness fraction. Bimonthly values are available and were related to monthly values as described on the NOAA-CDC website. To represent volcanic activity, we use the stratospheric aerosol optical thickness, a measure of the aerosols resulting from volcanic eruptions [*Sato et al.*, 1993] (available at http://data.giss.nasa.gov/modelforce/strataer/). The covariate effects are presented in Figures 1c and 1d.

3. Methodology

3.1. Change Point Detection

[11] The change point detection method used in this study can detect several types of changes and can be used to identify the most appropriate model from a range of candidates. The equations representing our candidate models are listed in Table 1 and illustrated in Figure 2. These models have been studied widely in the statistical and climate literature [e.g., *Quandt*, 1958; *Brown et al.*, 1975; *Worsley*, 1979; *Easterling and Peterson*, 1995; *Lund and Reeves*, 2002; *Chen and Gupta*, 1999, 2000, 2001; *Wang*, 2003; *Lund et al.*, 2007].

[12] To determine the position of the shift and to discriminate between these models, we use a methodology based on the informational approach proposed by *Chen and Gupta* [2000, 2001]. It consists of using the SIC which is based on the maximum likelihood function of a given model penalized by the number of parameters that are estimated in the model. In this study, we use the SIC to identify the position of the shift under a change point model formulation and to determine whether a model with or without a change point fits the data better. The model that minimizes the SIC can be considered as the most appropriate model [*Chen and Gupta*, 2000]. Here, the SIC is used as a measure for model selection among several models with different numbers of parameters. Because increasing the number of model parameters to be estimated may result in over fitting the data, SIC has a penalty term for the number of model parameters. The difference between the SIC and the Akaike Information Criterion (AIC) is the penalty term for the number of parameters to estimate, with a stronger penalty in the SIC. In the climate literature, the SIC has been used by *Seidel and Lanzante* [2004] to discriminate between several change point models to represent atmospheric temperature time series. In the present study, the SIC was used to search for the change point position in the models that include a change point, by calculating the SIC for each possible time for a change point. Then, the most likely position is the one that leads to the smallest SIC. The SIC was also used to discriminate between several models with different types of shifts or without a shift (the most likely model is the one which minimizes SIC). Further details on the statistical methodology are presented in Appendix A.

[13] Due to the large inter-annual variability in the estimated net land uptake, it is not clear from visual inspection alone whether the shift reported by *Sarmiento et al.* [2010] takes the form of a shift in the mean state, a long-term linear trend, or some combination of the two (Figure 1a). Therefore, all the models listed in Table 1 were fitted to the net land uptake in order to objectively determine the nature of the shift. In a preliminary analysis, models with shift in the variance were also fitted, but did not seem likely for the net land uptake, as they led to higher SIC.

[14] By visual inspection, Figure 1b suggests that there was a linear trend in the atmospheric growth rate with a possible shift in the intercept or both the intercept and trend in the late 1980s. Thus, the models iii, iv, v (Table 1) are also

Table 1. List of Models Fitted in This Study

Model	Description	Equations
(i)	Constant mean	$y_t = \mu + \varepsilon_t\ (t = 1,\ldots,n)$ where y_t represents the observations, μ is the mean, ε_t are the random errors, t is the time and n is the number of observations.
(ii)	Shift in the mean	$y_t = \begin{cases} \mu_1 + \varepsilon_t\ (t = 1,\ldots,p) \\ \mu_2 + \varepsilon_t\ (t = p+1,\ldots,n) \end{cases}$ where μ_1 and μ_2 are the means before and after the shift at time p
(iii)	Intercept and linear trend	$y_t = \lambda + \beta t + \varepsilon_t\ (t = 1,\ldots,n)$ where λ is the intercept, β the trend of the linear regression model,
(iv)	Shift in the intercept and same linear trend	$y_t = \begin{cases} \lambda_1 + \beta t + \varepsilon_t\ (t = 1,\ldots,p) \\ \lambda_2 + \beta t + \varepsilon_t\ (t = p+1,\ldots,n) \end{cases}$ λ_1 and λ_2 are the intercept before and after the shift
(v)	Shift in both the intercept and linear trend	$y_t = \begin{cases} \lambda_1 + \beta_1 t + \varepsilon_t\ (t = 1,\ldots,p) \\ \lambda_2 + \beta_2 t + \varepsilon_t\ (t = p+1,\ldots,n) \end{cases}$ β_1 and β_2 are the trend before and after the shift
(vi)	Intercept and linear relation with ENSO and optical thickness	$y_t = \lambda + \eta MEI_t + \tau OT_t + \varepsilon_t\ (t = 1,\ldots,n)$ η and τ are the regression coefficients for the multivariate ENSO index, MEI_t, and the optical thickness, OT_t
(vii)	Shift in the intercept and linear relation with ENSO and optical thickness	$y_t = \begin{cases} \lambda_1 + \eta MEI_t + \tau OT_t + \varepsilon_t\ (t = 1,\ldots,p) \\ \lambda_2 + \eta MEI_t + \tau OT_t + \varepsilon_t\ (t = p+1,\ldots,n) \end{cases}$

fitted to the atmospheric growth rate. However, the ocean uptake and the fossil fuel emissions, analyzed in a preliminary analysis, did not exhibit a shift in the late 1980s. Thus, these results are not presented in this study.

3.2. Integrating Covariate Effects in the Change Point Model

[15] The variability in the net land uptake estimates comes primarily from the variability of the atmospheric CO_2 growth rate. Variability in the ocean uptake (Figure 1a) and in the fossil fuel emissions (Figure 1b) is much smaller. A large part of the variability of the atmospheric CO_2 growth rate can be explained by ENSO and volcanic eruptions [*Conway et al.*, 1994; *Keeling et al.*, 1995; *Jones and Cox*, 2005; *Canadell et al.*, 2007; *Raupach et al.*, 2008; *Knorr*, 2009]. In order to verify whether there are still change points after accounting for ENSO and the volcanic eruptions, we extended the change point multiple linear regression models to integrate these covariate effects. We assume that the relationship between the net land uptake and these covariates is linear. We then evaluate whether the temporal shifts and variability in the net land uptake can be explained in terms of a linear relationship to ENSO, volcanic eruptions, and random noise, or if there is a remaining abrupt shift in the residuals. An abrupt shift in the residuals would indicate that there is still a shift in the net land uptake that cannot be explained by linear covariate effects. This result can be expressed as a shift in the intercept of a multiple linear regression model, which is equivalent to a shift in the mean (model ii) after explaining a part of the variability coming from ENSO and volcanic eruptions. To represent ENSO, we use the MEI (described in section 2.3). The optical thickness was used to represent the volcanic eruptions in the model. We take the relationship between the dependent variable and the covariate effects to be constant in time. Although our analysis can be extended to search for a change point in the parameters representing the relation with the covariates, for the sake of simplicity we restrict the analysis to search for a shift in the intercept. If a shift in the relationship with the explanatory variables occurred, we expect that it would come out as a shift in the intercept. The models including covariate effects fitted to the net land uptake are presented in Table 1 (models vi and vii). Furthermore, a summary of all the regression models used in this work and their associated SIC is presented in Table A1 in Appendix A.

[16] We attempted several other generalizations of the model. For example, if the response of the dependent variable to these covariate effects is lagged [e.g., *Lean and Rind*, 2009], it is necessary to find the appropriate lags for the explanatory variables. For the present work, no lag in the explanatory variables led to a better correlation. Second, we also took the solar irradiance to be another candidate explanatory variable. However, after a preliminary analysis using the total solar irradiance reaching the Earth's surface record from *Lean et al.* [2005], it was found that the models including solar irradiance were less appropriate (according to the SIC) to represent the net land uptake. Thus, models including the solar irradiance as an explanatory variable are not presented in this work.

[17] Since the explanatory variables all have different units of measurement, one cannot compare their effects on the dependent variable. However, we computed standardized coefficients by also fitting the model to standardized land

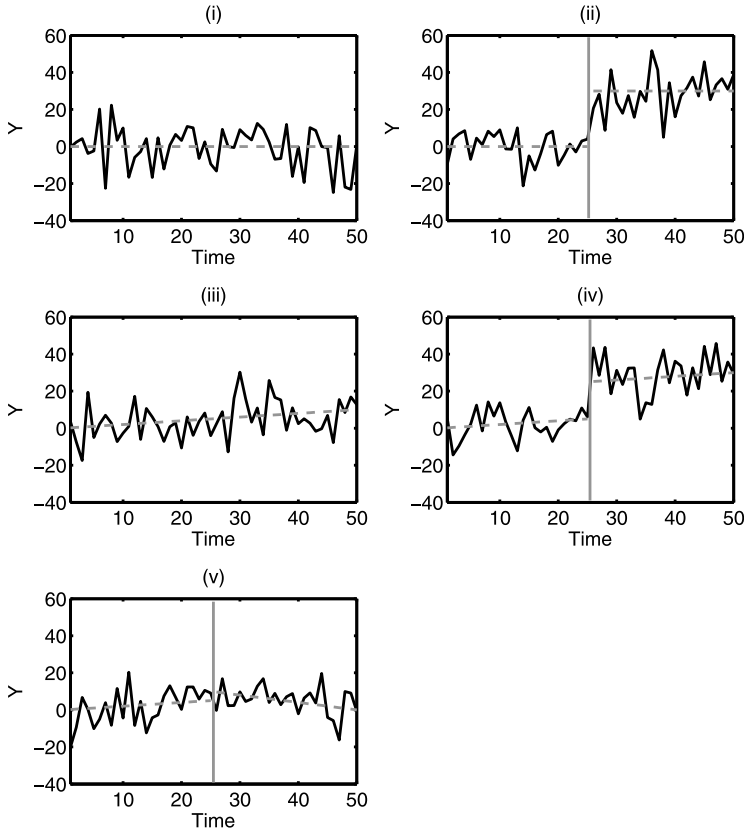

Figure 2. Examples of synthetic series generated from models fitted in this study (i) a constant mean and standard deviation ($\mu = 0$, $\sigma = 10$), (ii) a shift in the mean at time 25 ($\mu_1 = 0$, $\mu_2 = 30$, $\sigma = 10$), (iii) a linear trend ($\lambda = 0$, $\beta = 0.2$), (iv) a linear trend with a shift in the intercept at time 25 ($\lambda_1 = 0$, $\lambda_2 = 20$, $\beta = 0.2$) and (v) a shift in both the intercept and trend ($\lambda_1 = 0$, $\lambda_2 = 20$, $\beta_1 = 0.2$, $\beta_2 = -0.4$). The vertical line indicates the time of the shift and the dotted line indicates the model fit.

uptake, ENSO and optical thickness time series. We standardized the three time series by subtracting from them their respective mean and dividing them by their respective standard deviation. This ensures they all have a mean of zero, a variance of one, and that they are unit-free. Standardized coefficients are computed for all the models including ENSO and optical thickness to assess their effects on the net land uptake. These coefficients represent the change in terms of the standard deviation in the dependent variable that results from a change of one standard deviation in one of the explanatory variables.

[18] Finally, it must be noted that all these models rely on the assumption that the errors are normally distributed and independent. To validate this assumption, the residuals are usually analyzed. In this study, normality and independence tests were applied to the residuals in order to ensure that these assumptions are fulfilled.

3.3. Simulation Scheme

[19] In order to assess the skill of the technique and the significance of the model selected against a model with no shift, a Monte Carlo study was carried out. Using a Normal distribution random generator, we generated synthetic series with the same statistical properties (length, mean and variance) as those calculated in the net land uptake estimate. The first set of synthetic series we generated contains a shift in the mean net land uptake in 1988. In the second set of synthetic series we generate, there is no shift in the mean net land uptake.

3.3.1. Synthetic Series Mimicking a Shift in the Mean Net Land Uptake in 1988

[20] To represent series exhibiting a shift such as detected in the mean net land uptake, we generated series from two different distributions for the period 1960–1988 and 1989–2003 that have the same statistical properties observed in the net land uptake for these two respective periods. If there is a shift in the mean net land uptake after 1988, the model with a shift in the mean (model ii of Table 1) should be selected in a strong majority of the synthetic series that were generated. This simulation scheme seems appropriate since the net land uptake observations can be considered independent and normally distributed (Lilliefors and Wald-Wolfowitz test, 95% confidence level). A total number of 10,000 synthetic series for Mauna Loa and South Pole were generated. In a preliminary analysis, the number of synthetic series was found to be largely sufficient for the results to converge. In the remaining parts of the paper, we will denote the set of synthetic series generated from these two distributions as the set #1.

3.3.2. Synthetic Series Mimicking a Constant Mean Net Land Uptake

[21] It is well known that most change point detection techniques tend to detect more false shifts at the beginning

Table 2. Results of the Change Point Analysis on the Net Land Uptake at Mauna Loa and South Pole[a]

Station	Period	Model	Time	SIC	Parameter Estimates[b]
Mauna Loa (SIO)	1960–2003	i, **ii**,	-, **1988**,	137.55, **134.90**[c] (0.15),	$\mu_1 = 0.28$, $\mu_2 = 1.10$,
		iii, iv, v	-, 1988, 1988	138.63, 138.15, 140.08	$\mu_1 - \mu_2 = -0.82$, $\sigma = 1.07$
South Pole (SIO)	1966–2003	i, **ii**,	-, **1987**,	117.08, **116.10**[c] (0.35),	$\mu_1 = 0.46$, $\mu_2 = 1.16$,
		iii, iv, v	-, 1987, 1988	118.80, 119.00, 122.36	$\mu_1 - \mu_2 = -0.70$, $\sigma = 1.04$

[a]The model number refers to the models listed in Table 1. The most likely model, its associated SIC, and time of shift are in bold. The p-value associated to the SIC difference between models i and ii is in parentheses. The p-values are the probabilities, under the hypothesis of a model with no-shift, of observing a difference between the models with a shift and models with no-shift at least as extreme as the observed difference. The smaller the p-value, the more significant the difference between the models is.
[b]The parameter estimates correspond to the model with the smallest SIC.
[c]Smallest SIC.

or end of the time series [*Wang et al.*, 2007]. In order to verify if the risk of false detection around 1988 is not higher than at other times, a second set (set #2) of synthetic series was randomly generated from a Normal distribution with a constant overall mean and variance based on the mean and variance of the net land uptake time series. Model i of Table 1, representing a constant mean, should be selected in this case. The different models listed in Table 1 were applied to the two sets of synthetic series and the associated SIC were calculated. This is also the set of synthetic series that we used to determine the p-values and determine the significance of the model selected against a model with no-shift. A p-value measures the amount (in terms of probability) of sample evidence in favor of rejecting a null hypothesis. Specifically in this case, it is the probability of observing a difference between the models with a shift and models with no-shift at least as extreme as the observed value. Details on how the p-values in our model selection processes are computed are presented in Appendix A.

4. Results

4.1. Net Land Carbon Uptake

[22] Table 2 presents the results of the change point analysis on the net land uptake computed using the mean of the four ocean models and the atmospheric growth rate at Mauna Loa and the South Pole. According to the SIC, the net land uptake computed with these stations remained constant for almost three decades and might have abruptly shifted after 1988 (with Mauna Loa data, p-value of 0.15) and after 1987 (with South Pole data, p-value of 0.35). The magnitude of the shift in the net land uptake calculated with Mauna Loa data is about 0.82 Pg C/yr and with South Pole data it is 0.70 Pg C/yr. Figure 3 presents the model selected for the two time series.

[23] All models were also fitted to set #1 of the synthetic series and the associated SIC was computed for each time series. The results are presented in Figure 4. According to the SIC, the model with a shift in the mean only (model ii) is selected in a strong majority of cases for both Mauna Loa (78.2%) and South Pole (71.5%). Figure 4 also presents the most likely time for a shift when a shift in the mean was selected. The model with a shift in the mean occurring between 1986 and 1993 is found in a strong majority of cases for both Mauna Loa (60.5%) and South Pole (55.4%), with 1988 being the most likely year for the shift for both Mauna Loa (19.4%) and South Pole (15.4%). For all the other years of the time series (different than 1988), the shifts are identified with frequencies smaller than 10% (Figure 4). These detection rates are small because the power of detection of change point techniques is sensitive to the magnitude of the shift. In general, the power of change point techniques drops for magnitudes of about one standard deviation or less [e.g., *Beaulieu et al.*, 2008]. Because the magnitude of the 1988 shift is smaller than the standard deviation of the time series (the standard deviation is about 1 for both Mauna Loa and South Pole, see Table 2), this shift is very hard to detect.

[24] Figure 5 presents the results of the simulation study on synthetic series set #2, generated with the overall mean and variance in the net land uptake, and representing the case where no shift should be detected. Figure 5 shows that the risk of detecting a shift in the mean, when in reality there is not, is quite high (40%). However, it is also shown that the false alarms occur mostly near the beginning and end of the time series. The year 1988 lies in the region where the risk of false alarm is the smallest with a risk of about 1.8% (both Mauna Loa and South Pole).

[25] Additional evidence for this shift in the net land uptake was also investigated by repeating the analysis using

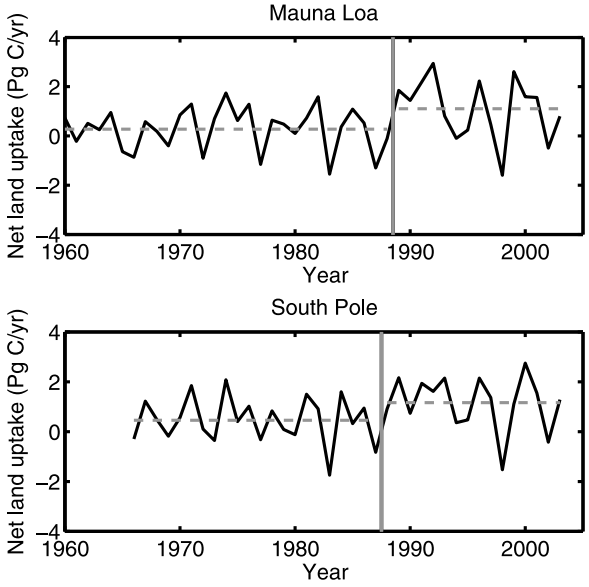

Figure 3. Fit of the model selected to explain the net land uptake at Mauna Loa and South Pole. The dotted lines represent the most appropriate model fit and the vertical lines indicate the time of the shift.

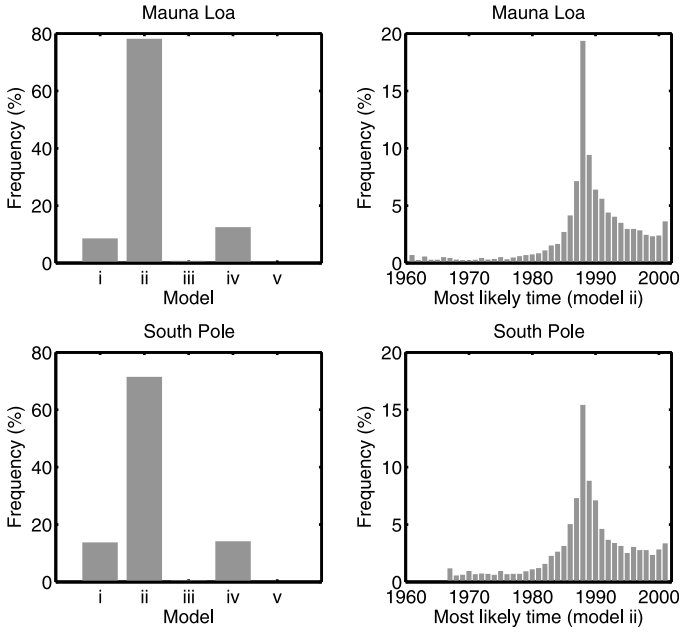

Figure 4. Results of the Monte Carlo study conducted on 5000 synthetic series generated with the same statistical properties (mean and variance) as the net land uptake at Mauna Loa and South Pole (set #1). (left) The frequency of model selected (constant mean (i), shift in the mean (ii), linear trend (iii), shift in the intercept (iv), shift in the intercept and trend (v)). (right) The most likely time for a shift, given the model with a shift in the mean (model ii) is selected.

CO_2 concentrations at other stations. Out of 11 stations analyzed, 4 showed a change point in 1988 (Appendix B). However, these 11 stations are generally not considered to be as representative of global growth rates as Mauna Loa and South Pole. Furthermore, the length of the record at these stations is shorter than those at Mauna Loa and South Pole and so the power of detection is lower and the risk of false detection is higher. The analysis performed on the net

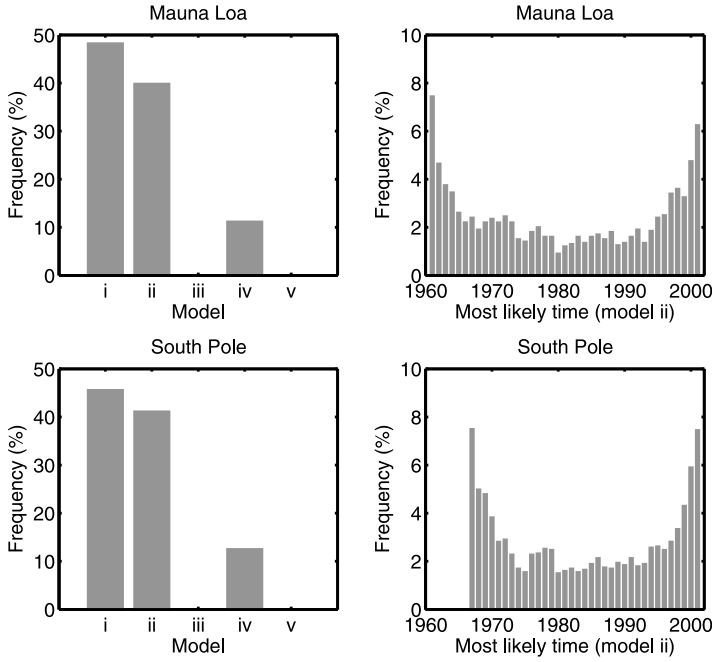

Figure 5. Results of the Monte Carlo study conducted on 5000 synthetic series generated to represent the same statistical properties of the net land uptake at Mauna Loa and South Pole, if they would not exhibit any shift (set #2). (left) The frequency of model selected (constant mean (i), shift in the mean (ii), linear trend (iii), shift in the intercept (iv), shift in the intercept and trend (v)). (right) The most likely time for a shift, given the model with a shift in the mean (model ii) is selected.

Table 3. Results of the Change Point Analysis on the Net Land Uptake at Mauna Loa and South Pole with Explanatory Variables[a]

Station	Period	Model	Time	SIC	Parameter	Parameter Estimates[b]	Parameter Estimates in Standardized Units
Mauna Loa (SIO)	1960–2003	vi, **vii**	-, **1988**	132.98, **118.67**[c] (0.01)	λ_1	−0.05	−0.37
					λ_2	1.11	0.72
					$\lambda_1 - \lambda_2$	−1.16	−1.09
					η	−0.88	−0.63
					τ	15.84	0.36
South Pole (SIO)	1966–2003	vi, **vii**	-, **1988**	115.94, **109.65**[c] (0.04)	λ_1	0.35	−0.35
					λ_2	1.27	0.53
					$\lambda_1 - \lambda_2$	−0.92	−0.88
					η	−0.76	−0.58
					τ	9.53	0.22

[a]Explanatory variables are Multivariate ENSO Index and optical thickness. The model number refers to the models listed in Table 1. The most likely model, its associated SIC and time of shift are in bold. The p-value associated to the SIC difference between models vi and vii is in parenthesis. The p-values are the probabilities, under the hypothesis of a model with no-shift, of observing a difference between the models with a shift and models with no-shift at least as extreme as the observed difference. The smaller the p-value, the more significant the difference between the models is.
[b]The parameter estimates correspond to the model with the smallest SIC.
[c]Smallest SIC.

land uptake calculated using the global growth rate from NOAA-ESRL also shows an abrupt shift in 1988.

4.2. Net Land Carbon Uptake With Covariate Effects

[26] The change point analysis was repeated including covariate effects with MEI and optical thickness in the model. The results of the fit to data are presented in Table 3. The analysis performed on the net land uptake shows that when accounting for a part of the variability using MEI and the optical thickness, it is likely that there is a remaining abrupt shift in the net land uptake, that is to say, that the intercept changes abruptly in 1988 (p-value of 0.01 for Mauna Loa and of 0.04 for the South Pole). The magnitude of this shift is 1.16 Pg C/yr (Mauna Loa) and 0.92 Pg C/yr (South Pole). The parameter estimates column in Table 3 presents the coefficients obtained by fitting the regression model to the standardized (0-mean and unit variance) variables. This allows comparison of the relative importance of each independent variable under the same units. Generally, an increase of a unit in MEI will more strongly affect the net land uptake than an increase of a unit of optical thickness. For example, the coefficients of the standardized parameters are respectively −0.63 units and 0.36 units for Mauna Loa. Figure 6 presents the fit of the selected model.

[27] Models vi and vii were also fitted to the synthetic series set #1 and the results are presented in Figure 7. The model with a shift in the intercept (model vii) was selected in 88.4% (Mauna Loa) and 83.4% (South Pole) of the synthetic series. Figure 7 also presents the most likely time for a shift identified by model vii in all the synthetic series. Once again, the most likely time for a shift is 1988. The most likely time for a shift lies between 1986 and 1993 in 60.0% (Mauna Loa) and 55.1% (South Pole) of the synthetic series.

4.3. Atmospheric Growth Rate

[28] Table 4 presents the results of the change point analysis of the annual growth rate of CO_2. According to the SIC, there is a shift in the intercept in 1988. The magnitudes of the shift are 1.34 Pg C/yr and 1.09 Pg C/yr for Mauna Loa and South Pole data respectively. The long-term linear trends are both 0.09 Pg C/yr^2. Figure 8 presents the fit of the model selected for each station.

5. Discussion

5.1. Comparison With Previous Results

[29] The shift detected in the mean net land uptake is in agreement with the results of *Sarmiento et al.* [2010], in which a shift of about 0.88 Pg C/yr was detected at the same time in the net land uptake computed using Mauna Loa observations with a confidence level of 99%. In the present study, however, the confidence obtained through Monte Carlo simulations is not as large as in the *Sarmiento et al.* [2010] analysis because the statistical analysis applied is different. We estimate the time of the shift using change point detection and discriminate among several models,

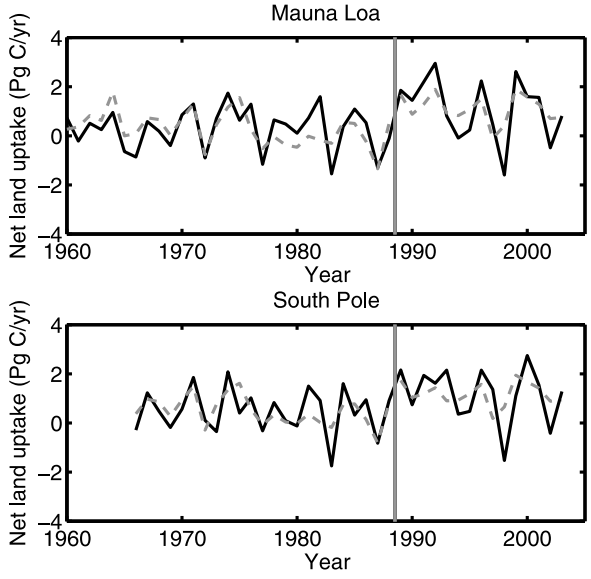

Figure 6. Fit of the model selected to explain the net land uptake at Mauna Loa and South Pole with explanatory variables (Multivariate ENSO Index and Optical thickness). The dotted lines represent the most appropriate model fit and the vertical lines indicate the time of the shift.

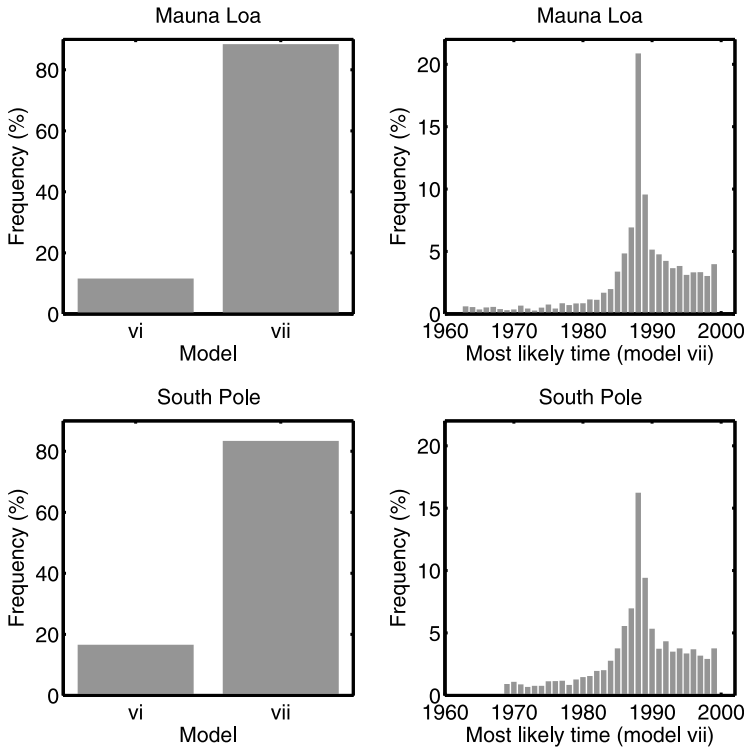

Figure 7. Results of the Monte Carlo study conducted on 5000 synthetic series generated with the same statistical properties (mean and variance) as the net land uptake at Mauna Loa and South Pole (set #1). (left) The frequency of the model selected (multiple linear regression model with covariates effects (vi), multiple linear regression model with covariate effects and a shift in the intercept (vii)). (right) The most likely time for a shift, given the model with a shift in the intercept (model vii) is selected.

whereas *Sarmiento et al.* [2010] applied a t-test to test whether the mean changes after 1988. Furthermore, in the work by *Sarmiento et al.* [2010], the decrease in the atmospheric growth rate was estimated to be approximately 0.53 Pg C/yr whereas we find a decrease of 1.34 Pg C/yr. The difference arises from the fact that *Sarmiento et al.* [2010] did not take into account the trend in the atmospheric CO_2 growth rate, whereas both temporal trends and shifts were modeled through linear regression in the present study.

5.2. Ocean Models and Data Uncertainties

[30] If uncertainties in the ocean uptake are sufficiently large, they can bias our inferences concerning terrestrial carbon uptake. However, when we applied our change point detection method to the net land uptake estimated using each ocean model separately, we detected the same shift, at the same time, in all the net land uptake estimates using the four ocean models and the two series of CO_2 atmospheric growth rate observations. We conclude that the detected shift is unaffected by uncertainty in ocean uptake, at least to the extent that the true ocean uptake is bracketed by the four models. Limitations common to all ocean models (e.g., coarse resolution, water formation, and inability to resolve eddies) were scrutinized by *Sarmiento et al.* [2010]. A comprehensive quantitative investigation of systematic uncertainties in forced ocean models is beyond the scope of this study, and left as a subject for future study. There is also data based information available about the ocean uptake [e.g., *Takahashi et al.*, 2009]. However, there is not sufficient spatiotemporal coverage of these data during the period prior to the shift in order to reliably use them to determine whether the shift may occur in the ocean fluxes.

[31] Artificial shifts are often introduced in climate data time series due to changes in measurement procedures or instrumentation at observation stations [e.g., *Peterson et al.*, 1998]. The growth rate time series is the time derivative of the atmospheric CO_2 accumulation. The growth rate for a given year is expressed as the difference in concentration

Table 4. Results of the Change Point Analysis on the Annual Atmospheric Growth Rate of CO_2 at Mauna Loa and South Pole[a]

Station	Period	Model	Time	SIC	Parameter Estimates[b]
Mauna Loa (SIO)	1960–2008	iii, **iv**, v	-, **1988**, 1988	147.72, **145.03**,[c] 148.89	$\lambda_1 = 1.22$, $\lambda_2 = -0.12$, $\lambda_1 - \lambda_2 = 1.34$, $\beta = 0.09$
South Pole (SIO)	1966–2008	iii, **iv**, v	-, **1988**, 1988	126.23, **125.98**,[c] 129.72	$\lambda_1 = 1.67$, $\lambda_2 = 0.58$, $\lambda_1 - \lambda_2 = 1.09$, $\beta = 0.09$

[a]The model number refers to the models listed in Table 1. The most likely model, its associated SIC and time of shift are in bold.
[b]The parameter estimates correspond to the model with the smallest SIC.
[c]Smallest SIC.

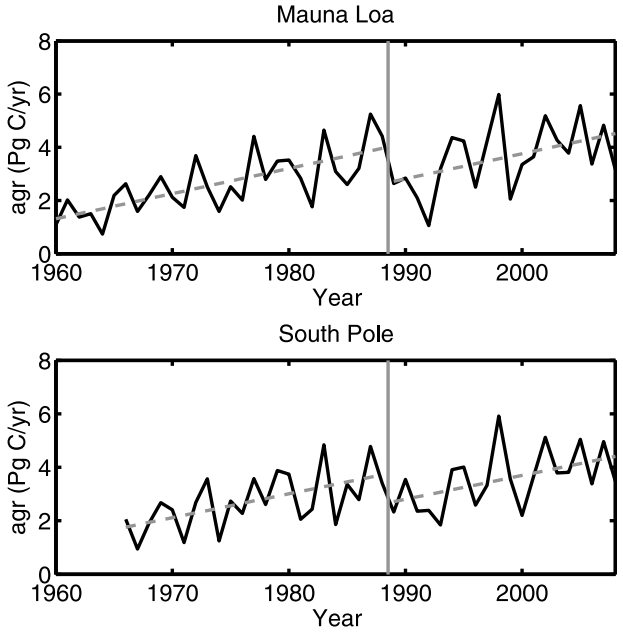

Figure 8. Fit of the model selected to explain the atmospheric CO_2 growth rate at Mauna Loa and South Pole. The dotted lines represent the model selected (according to the SIC) and the vertical lines indicate the time of the shift.

between the end of December and the start of January of that year. Thus, a mean shift in the CO_2 concentrations due to change of measurement procedures or instrumentation in 1988 would affect only the growth rate in that year, as opposed to the growth rate of all the years after the change (from 1989 to 2008), as observed in the results of this study. Thus, the possibility that this shift was introduced by a change of measurement procedures or instrumentation is unlikely.

5.3. Change Point Technique

[32] The change point technique based on the informational approach used in this study is advantageous because it allows us to discriminate among several types of models (normal model, linear regression model, and multiple linear regression model) and to integrate several explanatory variables in the change point models. However, there is no significance level involved in this approach: the smaller the SIC value of a model is, among many possible models, the better the likelihood is for the data being described by that model. Thus, to quantify the power and risk of false detection associated to this technique, we performed Monte Carlo simulation on synthetic series reflecting the properties of the net land uptake computed using Mauna Loa and South Pole data.

[33] This approach could also be extended in order to search for other types of changes, such as changes in the relationship (linear or nonlinear relationship, given the form of the relationship is known) between the net land uptake of carbon and their respective explanatory variables. This approach would also be useful for applications to other time series of observations or model estimates of atmospheric or climatic variables, in which one needs to discriminate between several types of models. It can be easily adapted and generalized to other problems.

[34] Finally, the change point approach applied was designed to detect at most one change point. The hypothesis that there is at most one change point seems reasonable here since we were interested in characterizing the most dominant shift. For different applications, this change point technique could be extended for the detection of multiple change points following an approach similar to that used by *Yao* [1988] or *Lu et al.* [2010].

6. Conclusions

[35] In this study, a change point analysis technique based on the SIC was applied to study shifts in the net land uptake of carbon. The atmospheric growth rate and the net land uptake were computed using CO_2 concentrations observed at Mauna Loa and South Pole. These two stations are often used to represent the global CO_2 concentrations. Our analysis shows that it is likely that a sudden increase in the mean of the net land uptake occurred in 1988. It seems unlikely that this shift is a false alarm because the risk of false detection around 1988 is small (about 2%). Our best estimate for the magnitude of this shift is 1.2 Pg C/yr (Mauna Loa) and 0.9 Pg C/yr (South Pole). This estimate takes into account the variability in the net land uptake driven by ENSO and by volcanic eruptions. The shift we detect is highly significant (p-values of 0.01 and 0.04 for South Pole and Mauna Loa, respectively) of the synthetic series. We confirm the shift in the net land uptake by detecting a simultaneous shift in the CO_2 atmospheric growth rate. According to the SIC, the CO_2 atmospheric growth rate exhibits a long-term linear trend that contains a sudden drop of about 1.3 Pg C/yr (Mauna Loa) and 1.1 Pg C/yr (South Pole) in 1988. We conclude that the most likely scenario is that a sudden increase in the land uptake occurred in 1988, leading to a corresponding decrease in the atmospheric CO_2 growth rate.

[36] More analysis is necessary in order to understand what could have caused this shift. Several candidates that could explain this shift were pointed out by *Sarmiento et al.* [2010]: an underestimate of the pre-1988/89 fossil fuel emissions or an overestimate of the post-1988/89 fossil fuel emissions, a decrease in land use emissions (not supported by existing publications), plant growth stimulation by climate variability such as the Atlantic Multidecadal Oscillation or the Pacific Decadal Oscillation, and many others. Understanding what caused this shift in the net land uptake is very important in order to eventually be able to predict future major shifts in the sources and sinks of carbon.

[37] To our knowledge, change point methods have not been used before to detect shifts in the carbon cycle. The technique presented here can easily be used to detect other types of changes in a regression model or in the parameters of the underlying distribution such as a shift in the mean and/or in the variance. It could be extended to search for shifts in the relationship between carbon cycle variables and explanatory variables representing the natural climate variability, the hydrological cycle, external forcings, etc. The change point approach presented in this paper is presently being extended to integrate the autocorrelation structure in order to study shifts at smaller time scales. Future work

should involve investigating shifts in the sources and sinks of atmospheric CO_2 at monthly time scale.

Appendix A

[38] In this appendix, we provide more details about the SIC formulation for the models fitted in this study. Details on how to obtain the SIC formulation for models iii-v are provided below. The SIC formulation can be obtained similarly for the other models and are summarized in Table A1.

[39] The general formulation of the SIC to select between models $j = 1,2,\ldots, m$ is given by:

$$SIC_j = -2\log L\left(\hat{\Theta}_j\right) + k_j \log n, \quad j = 1, 2, \ldots, m \tag{A1}$$

where SIC_j is the Schwarz Information Criterion for model j, $L(\hat{\Theta}_j)$ is the maximum likelihood function for the estimated model j, k_j is the number of parameters to be estimated for model j and n is the number of observations.

[40] In the regression model with no change point (model iii) and assuming the residuals are independent and normally distributed, the SIC can be expressed as:

$$SIC_{iii} = -2\log L\left(\hat{\lambda}, \hat{\beta}, \hat{\sigma}^2\right) + 3\log n \tag{A2}$$

$$L\left(\hat{\lambda}, \hat{\beta}, \hat{\sigma}^2\right) = \prod_{t=1}^{n} \frac{1}{\sqrt{2\pi\hat{\sigma}^2}} \exp\left\{-\left(y_t - \hat{\lambda} - \hat{\beta}t\right)^2 / 2\hat{\sigma}^2\right\} \tag{A3}$$

$$\hat{\sigma}^2 = \sum_{t=1}^{n} \left(y_t - \hat{\lambda} - \hat{\beta}t\right)^2 / n \tag{A4}$$

with $\hat{\lambda}$, $\hat{\beta}$ and $\hat{\sigma}^2$ being the maximum likelihood estimates of the intercept λ, the linear trend β and the error variance σ^2 in the regression model. The number 3 represents the number of parameters to estimate (intercept, trend and variance). By plugging equation (A4) and equation (A3) into equation (A2) and making some simplifications, we obtain:

$$SIC_{iii} = n\log(RSS_1) + n(1 + \log(2\pi)) + (3 - n)\log(n) \tag{A5}$$

where $RSS_1 = \sum_{t=1}^{n} \left(y_t - \hat{\lambda} - \hat{\beta}t\right)^2$ is the residual sum of squares of the model. Under the hypothesis that there is a shift in the intercept only (model iv), there is one additional parameter to estimate and the SIC becomes:

$$SIC_{iv}(k) = -2\log L\left(\hat{\lambda}_1, \hat{\lambda}_2, \hat{\beta}, \hat{\sigma}^2\right) + 4\log n \tag{A6}$$

$$L\left(\hat{\lambda}_1, \hat{\lambda}_2, \hat{\beta}, \hat{\sigma}^2\right) = \prod_{t=1}^{k} \frac{1}{\sqrt{2\pi\hat{\sigma}^2}} \exp\left\{-\left(y_t - \hat{\lambda}_1 - \hat{\beta}t\right)^2 / 2\hat{\sigma}^2\right\} \cdot \prod_{t=k+1}^{n} \frac{1}{\sqrt{2\pi\hat{\sigma}^2}} \exp\left\{-\left(y_t - \hat{\lambda}_2 - \hat{\beta}t\right)^2 / 2\hat{\sigma}^2\right\} \tag{A7}$$

$$\hat{\sigma}^2 = \left[\sum_{t=1}^{k} \left(y_t - \hat{\lambda}_1 - \hat{\beta}t\right)^2 + \sum_{t=k+1}^{n} \left(y_t - \hat{\lambda}_2 - \hat{\beta}t\right)^2\right] \Big/ n \tag{A8}$$

where $\hat{\lambda}_1$ and $\hat{\lambda}_2$ are the maximum likelihood estimates of the intercept before (λ_1) and after (λ_2) the shift at time k in the regression model. Again, by plugging equation (A8) and equation (A7) into equation (A6) and doing simplifications, we get:

$$SIC_{iv}(k) = n\log(RSS_2) + n(1 + \log(2\pi)) + (4 - n)\log(n) \quad k = 2, \ldots, n-2 \tag{A9}$$

where $RSS_2 = \sum_{t=1}^{k} \left(y_t - \hat{\lambda}_1 - \hat{\beta}t\right)^2 + \sum_{t=k+1}^{n} \left(y_t - \hat{\lambda}_2 - \hat{\beta}t\right)^2$. The SIC is evaluated for each possible time for a change point, from time 3 to $n - 2$, to ensure that there are at least as many observations as parameters to estimate on each side of the shift. Finally, under the hypothesis that there is a shift in both the intercept and trend (model v), the SIC is:

$$SIC_v(k) = -2\log L\left(\hat{\lambda}_1, \hat{\lambda}_2, \hat{\beta}_1, \hat{\beta}_2, \hat{\sigma}^2\right) + 5\log n \tag{A10}$$

$$L\left(\hat{\lambda}_1, \hat{\lambda}_2, \hat{\beta}_1, \hat{\beta}_2, \hat{\sigma}^2\right) = \prod_{t=1}^{k} \frac{1}{\sqrt{2\pi\hat{\sigma}^2}} \exp\left\{-\left(y_t - \hat{\lambda}_1 - \hat{\beta}_1 t\right)^2 / 2\hat{\sigma}^2\right\} \cdot \prod_{t=k+1}^{n} \frac{1}{\sqrt{2\pi\hat{\sigma}^2}} \exp\left\{-\left(y_t - \hat{\lambda}_2 - \hat{\beta}_2 t\right)^2 / 2\hat{\sigma}^2\right\} \tag{A11}$$

$$\hat{\sigma}^2 = \left[\sum_{t=1}^{k} \left(y_t - \hat{\lambda}_1 - \hat{\beta}_1 t\right)^2 + \sum_{t=k+1}^{n} \left(y_t - \hat{\lambda}_2 - \hat{\beta}_2 t\right)^2\right] \Big/ n \tag{A12}$$

where $\hat{\beta}_1$ and $\hat{\beta}_2$ are the maximum likelihood estimates of the trend before (β_1) and after (β_2) the shift at time k in the regression model. By plugging equation (A12) and equation (A11) into equation (A10) and simplifying, we get this expression:

$$SIC_v(k) = n\log(RSS_3) + n(1 + \log(2\pi)) + (5 - n)\log(n) \quad k = 2, \ldots, n-2 \tag{A13}$$

where RSS_3 is the residual sum of squares of the model with a shift both in the intercept and trend and is given by $RSS_3 = \sum_{t=1}^{k} \left(y_t - \hat{\lambda}_1 - \hat{\beta}_1 t\right)^2 + \sum_{t=k+1}^{n} \left(y_t - \hat{\lambda}_2 - \hat{\beta}_2 t\right)^2$. The time of the most likely shift (p) is determined by $SIC_v(p) = \min\{SIC_v(k),\ k = 2,\ldots,n-2\}$. Then, a model with a change after time p is selected if $SIC_v(p) < SIC_{iii}$ or if $SIC_{iv}(p) < SIC_{iii}$. Otherwise, it seems more likely that there is no shift in the model. Similarly, the SIC can be computed for the different models with or without a change point that are presented in Table 1. The SIC formulation has to be modified according to the number of parameters to estimate and to the residual sum of squares of each respective model. Furthermore, the time for which the SIC is computed has to be modified to make sure there are at least as many observations as parameters to estimate on each side of the shift. The SIC equations for all the models used in this study are presented in Table A1.

Table A1. List of Models Fitted in This Study With the Associated SIC Formulation

Model	Description	Equations
(i)	Constant mean	$y_t = \mu + \varepsilon_t \ (t = 1,\ldots,n)$ $SIC_i = n\log(RSS) + n(1 + \log(2\pi)) + (2 - n)\log(n)$
(ii)	Shift in the mean	$RSS = \sum_{t=1}^{n} (y_t - \bar{y})^2$, where $\bar{y}$ is the sample mean $y_t = \begin{cases} \mu_1 + \varepsilon_t \ (t = 1,\ldots,p) \\ \mu_2 + \varepsilon_t \ (t = p+1,\ldots,n) \end{cases}$ $SIC_{ii}(p) = n\log(RSS) + n(1 + \log(2\pi)) + (3 - n)\log(n)$ $RSS = \sum_{t=1}^{p} (y_t - \bar{y}_1)^2 + \sum_{t=p+1}^{n} (y_t - \bar{y}_2)^2$, where $\bar{y}_1$ and $\bar{y}_2$ are respectively the sample means before and after the shift
(iii)	Intercept and linear trend	$y_t = \lambda + \beta t + \varepsilon_t \ (t = 1,\ldots,n)$ $SIC_{iii} = n\log(RSS) + n(1 + \log(2\pi)) + (3 - n)\log(n)$
(iv)	Shift in the intercept and same linear trend	$RSS = \sum_{t=1}^{n} (y_t - \hat{\lambda} - \hat{\beta}t)^2$ $y_t = \begin{cases} \lambda_1 + \beta t + \varepsilon_t \ (t = 1,\ldots,p) \\ \lambda_2 + \beta t + \varepsilon_t \ (t = p+1,\ldots,n) \end{cases}$ $SIC_{iv}(p) = n\log(RSS) + n(1 + \log(2\pi)) + (4 - n)\log(n)$
(v)	Shift in both the intercept and linear trend	$RSS = \sum_{t=1}^{p} (y_t - \hat{\lambda}_1 - \hat{\beta}t)^2 + \sum_{t=p+1}^{n} (y_t - \hat{\lambda}_2 - \hat{\beta}t)^2$ $y_t = \begin{cases} \lambda_1 + \beta_1 t + \varepsilon_t \ (t = 1,\ldots,p) \\ \lambda_2 + \beta_2 t + \varepsilon_t \ (t = p+1,\ldots,n) \end{cases}$ $SIC_v(p) = n\log(RSS) + n(1 + \log(2\pi)) + (5 - n)\log(n)$
(vi)	Intercept and linear relation with ENSO and optical thickness	$RSS = \sum_{t=1}^{p} (y_t - \hat{\lambda}_1 - \hat{\beta}_1 t)^2 + \sum_{t=p+1}^{n} (y_t - \hat{\lambda}_2 - \hat{\beta}_2 t)^2$ $y_t = \lambda + \eta MEI_t + \tau OT_t + \varepsilon_t \ (t = 1,\ldots,n)$ $SIC_{vi} = n\log(RSS) + n(1 + \log(2\pi)) + (4 - n)\log(n)$
(vii)	Shift in the intercept and linear relation with ENSO and optical thickness	$RSS = \sum_{t=1}^{n} (y_t - \hat{\lambda} - \hat{\eta}MEI_t - \hat{\tau}OT_t)^2$ $y_t = \begin{cases} \lambda_1 + \eta MEI_t + \tau OT_t + \varepsilon_t \ (t = 1,\ldots,p) \\ \lambda_2 + \eta MEI_t + \tau OT_t + \varepsilon_t \ (t = p+1,\ldots,n) \end{cases}$ $SIC_{vii}(p) = n\log(RSS) + n(1 + \log(2\pi)) + (5 - n)\log(n)$ $RSS = \sum_{t=1}^{p} (y_t - \hat{\lambda}_1 - \hat{\eta}MEI_t - \hat{\tau}OT_t)^2 + \sum_{t=p+1}^{n} (y_t - \hat{\lambda}_2 - \hat{\eta}MEI_t - \hat{\tau}OT)^2$

[41] There is no significance level involved with the decision rule presented above. To assess significance, a critical value can be included in the decision rule. For example, when comparing model i and ii, model ii will be selected if $SIC_{ii}(p) + c_\alpha < SIC_i$, with c_α being the critical value at the α significance level. In this paper, we obtain the critical values and associated significance levels by Monte Carlo simulations. More specifically, we use the set of synthetic series mimicking a constant mean net land uptake presented in section 3.3.2. For each synthetic series, we fit models i and ii, compute the associate SIC values (SIC_i and $SIC_{ii}(p)$) and their difference. These differences give an estimate of the distribution of c_α under a model with no-shift in the mean net land uptake. The value that is larger than 95% of the other values is the critical value associated to within a 5% significance level. The significance for a shift in the net land uptake observations can be obtained by comparing the difference between the SIC of a model with a shift and a model with no-shift to the critical value at a desired significance level (e.g., the common 5% level). If this difference is larger than the critical value for the 5% significance level approximated by Monte Carlo, the associated p-value is smaller than 0.05 and the hypothesis that there is no shift in the mean net land uptake can be rejected. In this context, the p-value represents the probability of observing a difference between the models with a shift and models with no-shift at least as extreme as the observed difference.

Appendix B

[42] In this appendix, we look for additional evidence for a shift in the net land carbon uptake in 1988/1989 by analyzing the net land uptake of carbon computed using the atmospheric CO_2 growth rate at several locations (Table B1). The longest publically available records of CO_2 concentration observations at several stations from SIO and NOAA-ESRL [*Thoning et al.*, 1989] (available at http://www.esrl.noaa.gov/gmd/ccgg/trends/) are used. The analysis is performed at the annual time scale at stations for which there are enough observations to compute the growth rate since at least 1980. In order to avoid spurious change point detection, we only included data from stations with observations from 1980 to 2008 or longer and that do no have gaps of 12 consecutive

Table B1. Results of the Change Point Analysis on the Annual Net Land Uptake at Several Stations[a]

Station	Period	Model	Time	SIC	Parameter Estimates[b]
La Jolla Pier (SIO)	1970–2003	**i**, ii, iii, iv, v	-, 2001, -, 1988, 1998	**141.70**,[c] 144.15, 145.21, 145.43, 147.95	$\mu = 0.75$, $\sigma = 1.78$
Point Barrow (SIO)	1975–2003	i, ii, iii, **iv**, v	-, 1988, -, **1988**, 1988	138.02, 140.00, 141.37, **137.72**,[c,d] 141.02	$\lambda_1 = 1.93$, $\lambda_2 = 6.25$, $\lambda_1 - \lambda_2 = -4.33$, $\beta = -0.23$
Christmas Island (SIO)	1976–2003	**i**, ii, iii, iv, v	-, 1988, -, 1988, 1977	**98.25**,[c] 99.39, 101.35, 100.04, 103.11	$\mu = 0.76$, $\sigma = 1.26$
Key Biscane (NOAA-ESRL)	1977–2003	**i**, ii, iii, iv, v	-, 1989, -, 1989, 1982	**107.50**,[c] 108.18, 110.16, 109.97, 110.96	$\mu = 0.61$, $\sigma = 1.60$
Niwot Ridge (NOAA-ESRL)	1977–2003	i, ii, iii, iv, **v**	-, 1988, -, 1988, **1979**	100.61, 100.77, 103.32, 101.73, **99.93**[c]	$\lambda_1 = -3.98$, $\lambda_2 = -0.16$, $\beta_1 = 2.56$, $\beta_2 = 0.05$
Baring Head (SIO)	1978–2003	**i**, ii, iii, iv, v	-, 1987, -, 1987, 1987	**82.65**,[c,d] 83.81, 85.85, 83.37, 86.12	$\mu = 0.88$, $\sigma = 1.07$
Palmer Station (NOAA-ESRL)	1979–2003	i, ii, iii. **iv**, v	-, 1988, -, **1988**, 1988	74.94, 72.79, 77.44, **70.83**,[c] 73.91	$\lambda_1 = 0.85$, $\lambda_2 = 2.92$, $\lambda_1 - \lambda_2 = -2.07$, $\beta = -0.10$
Cape Kumukahi (SIO)	1980–2003	**i**, ii, iii, iv, v	-, 1989, -, 1989, 1989	**83.41**,[c] 84.92, 86.47, 85.81, 88.95	$\mu = 0.80$, $\sigma = 1.23$
Cold Bay (NOAA-ESRL)	1980–2003	**i**, ii, iii, iv, v	-, 2001, -, 1988, 1988	**96.71**,[c] 97.34, 99.75, 97.93, 101.11	$\mu = 0.71$, $\sigma = 1.62$
Mariana Islands (NOAA-ESRL)	1980–2003	i, ii, iii, **iv**, v	-, 1988, -, **1988**, 1988	90.25, 90.88, 93.42, **87.30**,[c] 90.17	$\lambda_1 = 1.13$, $\lambda_2 = 4.13$, $\lambda_1 - \lambda_2 = -2.99$, $\beta = -0.17$
Global (NOAA-ESRL)	1980–2003	i, ii, iii, **iv**, v	-, 1988, -, **1988**, 1988	84.55, 84.24, 87.45, **83.24**,[c] 86.38	$\lambda_1 = 0.82$, $\lambda_2 = 3.22$, $\lambda_1 - \lambda_2 = -2.40$, $\beta = -0.12$

[a]The model number refers to the models listed in Table 1. The most likely model, its associated SIC and time of shift are in bold.
[b]The parameter estimates correspond to the model with the smallest SIC.
[c]Smallest SIC.
[d]The normality hypothesis is not respected (Lilliefors test, 95% confidence level).

months or more in the CO_2 record. If there are gaps of 12 months or longer at the beginning of the record, we leave out these years and use only the remaining part of the record for which there is no long gap. In addition, we analyzed the global time series calculated by NOAA-ESRL by combining their stations to produce a globally representative time series.

[43] We found that it is likely that a shift occurred in 1988 in 4 stations out of 11. Most of these stations are not as representative for global growth rates as Mauna Loa or the South Pole. It should be noted that the analysis performed using the global growth rate from NOAA-ESRL also shows an abrupt shift in 1988.

[44] **Acknowledgments.** The authors would like to thank G. Stenchikov for helping with the optical thickness record; G. Marland for providing the fossil fuel emissions estimates; R. Keeling, S. Piper, and P. Tans for providing the CO_2 concentration observations freely on the Internet; and K. Wolter for providing the Multivariate ENSO Index data freely on the Internet. The authors would also like to thank J. Lean for providing the solar irradiance data that was used in preliminary analyses. The authors would like to thank W. Buermann, M. Gloor, and J. Lanzante for useful comments on the manuscript. The authors would also like to thank I. Enting, an anonymous reviewer, the Associate Editor, and the Editor for making valuable comments that improved the quality of the paper. The authors acknowledge financial support from the Fonds Québécois de la Recherche sur la Nature et les technologies, the Carbon Mitigation Initiative with support from BP, the Cooperative Institute for Climate Science, and the New Zealand Research Foundation (contract C01X0703).

References

Beaulieu, C., O. Seidou, T. B. M. J. Ouarda, X. Zhang, G. Boulet, and A. Yagouti (2008), Intercomparison of homogenization techniques for precipitation data, *Water Resour. Res.*, *44*, W02425, doi:10.1029/2006WR005615.

Boden, T. A., G. Marland, and R. J. Andres (2009), Global, Regional, and national fossil-fuel CO_2 emissions, report, Carbon Dioxide Inf. Anal. Cent., Oak Ridge Natl. Lab, U.S. Dep. of Energy, Oak Ridge, Tenn., doi:10.3334/CDIAC/00001.

Brown, R. L., J. Durbin, and J. M. Evans (1975), Techniques for testing the consistency of regression relationships over time, *J. R. Stat. Soc., B*, *37*(2), 149–192.

Canadell, J. G., C. Le Quéré, M. R. Raupach, C. B. Field, E. T. Buitenhuis, P. Ciais, T. C. Conway, N. P. Gillett, R. A. Houghton, and G. Marland (2007), Contributions to accelerating atmospheric CO_2 growth from economic activity, carbon intensity, and efficiency of natural sinks, *Proc. Natl. Acad. Sci. U. S. A.*, *104*(47), 18,866–18,870, doi:10.1073/pnas.0702737104.

Chen, J., and A. K. Gupta (1997), Testing and locating variance change points with application to stock prices, *J. Am. Stat. Assoc.*, *92*, 739–747, doi:10.2307/2965722.

Chen, J., and A. K. Gupta (1999), Change point analysis of a Gaussian model, *Statist. Papers*, *40*, 323–333, doi:10.1007/BF02929878.

Chen, J., and A. K. Gupta (2000), *Parametric Statistical Change-Point Analysis*, 183 pp., Birkhauser, Boston, Mass.

Chen, J., and A. K. Gupta (2001), On change-point detection and estimation, *Comm. Statist. Simulation Comput.*, *30*(3), 665–697, doi:10.1081/SAC-100105085.

Conway, T. J., P. P. Tans, L. S. Waterman, K. W. Thoning, D. R. Kitzis, K. A. Masarie, and N. Zhang (1994), Evidence for interannual variability of the carbon cycle from the National Oceanic and Atmospheric Administration/Climate Monitoring and Diagnostics Laboratory Global Air Sampling Network, *J. Geophys. Res.*, *99*(D11), 22,831–22,855, doi:10.1029/94JD01951.

Easterling, D. R., and T. C. Peterson (1995), A new method for detecting undocumented discontinuities in climatological time series, *Int. J. Climatol.*, *15*(4), 369–377, doi:10.1002/joc.3370150403.

Hanley, D. E., M. A. Bourassa, J. J. O'Brien, S. R. Smith, and E. R. Spade (2003), A quantitative evaluation of ENSO indices, *J. Clim.*, *16*, 1249–1258, doi:10.1175/1520-0442(2003)16<1249:AQEOEI>2.0.CO;2.

Jandhyala, V. K., and I. B. MacNeill (1991), Tests for parameter changes at unknown times in linear regression models, *J. Statist. Plann. Inference*, *27*, 291–316, doi:10.1016/0378-3758(91)90043-E.

Jones, C. D., and P. M. Cox (2001), Modeling the volcanic signal in the atmospheric CO_2 record, *Global Biogeochem. Cycles*, *15*(2), 453–465, doi:10.1029/2000GB001281.

Jones, C. D., and P. M. Cox (2005), On the significance of atmospheric CO_2 growth rate anomalies in 2002–2003, *Geophys. Res. Lett.*, *32*, L14816, doi:10.1029/2005GL023027.

Keeling, C. D., T. P. Whorf, M. Wahlen, and J. van der Plicht (1995), Interannual extremes in the rate of rise of atmospheric carbon dioxide since 1980, *Nature*, *375*, 666–670, doi:10.1038/375666a0.

Keeling, C. D., S. C. Piper, R. B. Bacastow, M. Wahlen, T. P. Whorf, M. Heimann, and H. A. Meijer (2001), Exchanges of atmospheric CO2 and 13CO2 with the terrestrial biosphere and oceans from 1978 to 2000. I. Global aspects, *SIO Ref. 01–06*, Scripps Inst. of Oceanogr., San Diego, Calif.

Knorr, W. (2009), Is the airborne fraction of anthropogenic CO_2 emissions increasing?, *Geophys. Res. Lett.*, *36*, L21710, doi:10.1029/2009GL040613.

Le Quéré, C., et al. (2007), Saturation of the Southern Ocean CO_2 sink due to recent climate change, *Science*, *316*, 1735–1738, doi:10.1126/science.1136188.

Le Quéré, C., et al. (2009), Trends in the sources and sinks of carbon dioxide, *Nat. Geosci.*, *2*, 831–836, doi:10.1038/ngeo689.

Lean, J. L., and D. R. Rind (2009), How will Earth's surface temperature change in future decades?, *Geophys. Res. Lett.*, *36*, L15708, doi:10.1029/2009GL038932.

Lean, J. L., G. Rottman, J. Harder, and G. Kopp (2005), SORCE contributions to new understanding of global change and solar variability, *Sol. Phys.*, *230*, 27–53, doi:10.1007/s11207-005-1527-2.

Lovenduski, N. S., N. Gruber, and S. C. Doney (2008), Towards a mechanistic understanding of the decadal trends in the Southern Ocean carbon sink, *Global Biogeochem. Cycles*, *22*, GB3016, doi:10.1029/2007GB003139.

Lu, Q., R. Lund, and T. C. M. Lee (2010), An MDL approach for the climate segmentation problem, *Ann. Appl. Stat.*, *4*(1), 299–319, doi:10.1214/09-AOAS289.

Lund, R., and J. Reeves (2002), Detection of undocumented changepoints: A revision of the two-phase regression model, *J. Clim.*, *15*(17), 2547–2554, doi:10.1175/1520-0442(2002)015<2547:DOUCAR>2.0.CO;2.

Lund, R., X. L. Wang, Q. Lu, J. Reeves, C. Gallagher, and Y. Feng (2007), Changepoint detection in periodic and autocorrelated time series, *J. Clim.*, *20*(20), 5178–5190, doi:10.1175/JCLI4291.1.

Peterson, T. C., et al. (1998), Homogeneity adjustments of in situ atmospheric climate data: A review, *Int. J. Climatol.*, *18*(13), 1493–1517, doi:10.1002/(SICI)1097-0088(19981115)18:13<1493::AID-JOC329>3.0.CO;2-T.

Quandt, R. E. (1958), The estimation of the parameters of a linear regression system obeying two separate regimes, *J. Am. Stat. Assoc.*, *53*(284), 873–880, doi:10.2307/2281957.

Raupach, M. R. (2011), Pinning down the land carbon sink, *Nat. Clim. Change*, *1*, 148–149, doi:10.1038/nclimate1123.

Raupach, M. R., J. G. Canadell, and C. Le Quéré (2008), Anthropogenic and biophysical contributions to increasing atmospheric CO_2 growth rate and airborne fraction, *Biogeosciences*, *5*, 1601–1613, doi:10.5194/bg-5-1601-2008.

Rodgers, K. B., J. L. Sarmiento, O. Aumont, C. Crevoisier, C. B. Montegut, and N. Metzl (2008), A wintertime uptake window for anthropogenic CO_2 in the North Pacific, *Global Biogeochem. Cycles*, *22*, GB2020, doi:10.1029/2006GB002920.

Sarmiento, J. L., and E. T. Sundquist (1992), Revised budget for the oceanic uptake of anthropogenic carbon dioxide, *Nature*, *356*, 589–593, doi:10.1038/356589a0.

Sarmiento, J. L., M. Gloor, N. Gruber, C. Beaulieu, A. R. Jacobson, S. Mikaloff Fletcher, S. Pacala, and K. Rodgers (2010), Trends and regional distributions of land and ocean sinks, *Biogeosciences*, *7*, 2351–2367, doi:10.5194/bg-7-2351-2010.

Sato, M., J. E. Hansen, M. P. McCormick, and J. B. Pollack (1993), Stratospheric aerosol optical depth, 1850–1990, *J. Geophys. Res.*, *98*, 22,987–22,994, doi:10.1029/93JD02553.

Schwarz, G. (1978), Estimating the dimension of a model, *Ann. Stat.*, *6*(2), 461–464, doi:10.1214/aos/1176344136.

Seidel, D. J., and J. R. Lanzante (2004), An assessment of three alternatives to linear trends for characterizing global atmospheric temperature changes, *J. Geophys. Res.*, *109*, D14108, doi:10.1029/2003JD004414.

Solow, A. R. (1987), Testing for climate change: An application of the two-phase regression model, *J. Clim. Appl. Meteorol.*, *26*(10), 1401–1405, doi:10.1175/1520-0450(1987)026<1401:TFCCAA>2.0.CO;2.

Takahashi, T., et al. (2009), Climatological mean and decadal change in surface ocean pCO_2, and net sea-air CO_2 flux over the global oceans, *Deep Sea Res., Part II*, *56*, 554–577, doi:10.1016/j.dsr2.2008.12.009.

Thoning, K. W., P. T. Tans, and W. D. Komhyr (1989), Atmospheric carbon dioxide at Mauna Loa observatory: 2. Analysis of the NOAA GMCC data, 1974–1985, *J. Geophys. Res.*, *94*(D6), 8549–8565, doi:10.1029/JD094iD06p08549.

Wang, X. L. (2003), Comments on 'Detection of undocumented changepoints: A revision of the two-phase regression model,' *J. Clim.*, *16*(20), 3383–3385, doi:10.1175/1520-0442(2003)016<3383:CODOUC>2.0.CO;2.

Wang, X. L., Q. H. Wen, and Y. Wu (2007), Penalized maximal t test for detecting undocumented mean change in climate data series, *J. Appl. Meteorol. Climatol.*, *46*(6), 916–931, doi:10.1175/JAM2504.1.

Wetzel, P., A. Winguth, and E. Maier-Reimer (2005), Sea-to-air CO_2 flux from 1948 to 2003: A model study, *Global Biogeochem. Cycles*, *19*, GB2005, doi:10.1029/2004GB002339.

Wolter, K., and M. S. Timlin (1993), Monitoring ENSO in COADS with a seasonally adjusted principal component index, in *Proceedings of the 17th Climate Diagnostics Workshop*, pp. 52–57, Univ. of Okla., Norman.

Wolter, K., and M. S. Timlin (1998), Measuring the strength of ENSO events: How does 1997/98 rank?, *Weather*, *53*, 315–324.

Worsley, K. J. (1979), On the likelihood ratio test for a shift in location of Normal populations, *J. Am. Stat. Assoc.*, *74*(366), 365–367, doi:10.2307/2286336.

Yao, Y.-C. (1988), Estimating the number of change-points via Schwarz criterion, *Stat. Probab. Lett.*, *6*(3), 181–189, doi:10.1016/0167-7152(88)90118-6.

C. Beaulieu, D. Medvigy, and J. L. Sarmiento, Program in Atmospheric and Oceanic Sciences, Princeton University, Sayre Hall, Forrestal Campus, 300 Forrestal Rd., Princeton, NJ 08540, USA. (beaulieu@princeton.edu)

J. Chen, Department of Mathematics and Statistics, University of Missouri at Kansas City, 206 Haag Hall, 5100 Rockhill Rd., Kansas City, MO 64110, USA.

S. E. Mikaloff Fletcher, National Institute of Water and Atmospheric Research, 301 Evans Bay Parade, Wellington 6022, New Zealand.